Response of a Nuclear Power Plant on Aseismic Bearings from Horizontally Propagating Waves

J.P. Wolf, P. Obernhuber, B. Weber
Electrowatt Engineering Services Ltd., Bellerivestr. 36, CH-8022 Zurich, Switzerland

SUMMARY

The nuclear island of Koeberg with a large basemat, a nonlinear base isolation effective in the horizontal direction only, founded on rock, is analysed for horizontally propagating waves. The horizontal and vertical components of the control motion are either associated with inclined P- and SV-waves or with a combination of a P-wave and the first two Rayleigh modes. The response is compared to that resulting from vertically incident waves. Although the analysis of soil-structure interaction uses the principle of superposition by performing first the free-field analysis and then the actual interaction calculation, the structure in the latter can exhibit nonlinear behaviour. The governing equation of motion in the time domain contains convolution integrals, which can be removed by assuming a frequency-independent dynamic-stiffness matrix of the unbounded soil.

It is demonstrated that the aseismic bearings result in a significant isolation in the horizontal direction for vertically incident waves. The vertical excitation affects considerably the response in the horizontal direction in the frequency range of the vertical modes for the nonlinear base isolation.

When compared to vertical incidence, the horizontal component of the propagating wave is filtered significantly because of the size of the raft. However, this results in only a slightly smaller structural response, since the aseismic bearings already represent a filter. The vertical response is hardly affected by horizontally propagating waves. An additional rocking component arises, generated by the horizontally propagating vertical component. As the aseismic bearings do not isolate against this rocking component, the corresponding horizontal response bears comparison with that of a conventional structure. For the base-isolated structure, the rocking input leads to a considerable increase of the horizontal response. The actual design incorporating other loading cases is affected much less. Horizontally travelling waves hardly modify the maximum horizontal displacements and the amount and duration of sliding. A larger variation of the vertical Neoprene forces occurs, but no uplift arises.

The complete paper will be published in Earthquake Engineering and Structural Dynamics (Vol. 11, 1983).

1. INTRODUCTION

Structures are routinely designed for vertically incident body waves. Assuming the wave pattern to consist of inclined body waves and of surface waves, the waves propagate horizontally across the site. The seismic input of a surface structure will in this case consist of (reduced) translational components and additional rotational components not present for vertical incidence. The effects of horizontally propagating waves on the seismic response of conventional structures of common dimensions have been evaluated systematically (Ref.1). Only for extreme assumptions of the wave pattern are these effects of importance, increasing generally for larger dimensions of the basemat. Structures which are isolated at the base in the horizontal direction only are examined in Reference 2. As the rocking component of the seismic input is not isolated in this concept, the effects of horizontally propagating waves are in general larger than in conventional structures. Along with the structural configuration, the properties of the site are of importance to evaluate wave-passage effects. For soft sites with large material damping, the surface waves attenuate significantly (Refs. 3,4). Thus in general, only rock sites have to be examined for horizontally propagating surface waves.

As the nuclear island of the Koeberg Nuclear Power Plant in South Africa has a large basemat, a horizontal isolation mechanism and is founded on rock, horizontally propagating waves are investigated. A schematic section passing through the nuclear island is shown in Figure 1. The isolation mechanism using aseismic bearings is well documented in the literature (e.g. Ref. 5,6,7). All safety-related structures of the nuclear island are founded on a common upper raft. The aseismic bearings are located between the lower and upper rafts. On top of concrete pedestals resting on the lower raft, Neoprene pads, which are flexible in the horizontal direction only, are placed. In addition, friction plates are used to limit the horizontal force transmitted to the structure. This results in a nonlinear isolation mechanism acting in the horizontal direction only. The lower raft rests on a layer of soil-cement which is on top of a layered rock site.

The nuclear island of Koeberg is analysed for horizontally propagating waves in Reference 8 , whereby a constant apparent velocity, selected conservatively, is assumed. A more realistic seismic input compatible with the equations of elastodynamics applied to the layered site is used in this article. For the sake of conciseness, the results of only one set of parameters (which do not necessarily govern the design) are presented. Horizontally propagating SH- and Love-waves are not analysed, as the horizontal isolation mechanism also acts for the additional torsional seismic input generated by these waves. A two-dimensional model is adopted for the analysis of the soil-structure interaction caused by SV-, P- and Rayleigh waves.

2. MODELLING OF STRUCTURE AND SOIL

The dynamic model of the nuclear island of Koeberg is shown schematically in Figure 2. A simple model is deliberately selected which, however, can represent the characteristic effects arising from horizontally propagating waves. For this purpose only three buildings are

included in the 2-dimensional model. The structures are modelled with beams and lumped masses. The upper raft consists of three rigid sections connected by two flexible parts. The lower raft is assumed to be flexible over the whole length. Both ratts are rigid in the horizontal direction. Each row of the aseismic bearings in the third dimension is modelled as a discrete element representing the horizontal and vertical flexibilities of the Neoprene pads and the friction plates. A total of 25 elements arise, which are not equally spaced. The pads are designed to exhibit a horizontal stiffness which results in a horizontal frequency = 0.9 Hz of the total system, assuming the upper ratt and the structures to be rigid and the lower raft fixed. The coefficient of friction equals 0.15. The lower ratt is founded on the layer of soil cement of 6 m thickness resting on bedrock. The latter is modelled with 10 homogeneous layers which rest on a homogeneous halfspace (-120 m). The material properties of the site are specified in Table I. The shear-wave velocity increases with depth, while the damping ratio of the bedrock is constant.

When analysing nonlinear soil-structure interaction by the substructure method, the nonlinearity has to be restricted to the structure. The unbounded soil must remain linear. The governing equations of motion are formulated using the nuclear island on nonlinear aseismic bearings shown in Figure 1 for illustration.

The interface of the lower raft and the soil is discretised with 25 substrips analogously to the elements modelling the aseismic bearings. Taking the constraints imposed by the rigid connections into account, the total dynamic model has 94 dynamic degrees of freedom.

The dynamic-stiffness matrix of the soil is of order 50 x 50. For a constant surface traction acting on each substrip, the dynamic-flexibility influence functions can be calculated by integrating for a specific frequency in the wave-number domain, which then leads to the dynamic-stiffness matrix (Refs. 9, 10). To examine the frequency dependency, the dynamic-stiffness coefficients in the vertical direction and for rocking of the total lower ratt of length 134.4 m, assumed to be rigid and massless, are evaluated. They are plotted in Figure 3 (nondimensionalised by the corresponding value at 9 Hz, treating the real and imaginary parts separately). Although the site is layered, the dependency on frequency in the range of interest is not overwhelming. The frequency selected for calculating the dynamic-stiffness matrix equals 9 Hz (As a check, other frequencies were also selected. The differences in the dynamic response were found to be defensible).

3. FREE-FIELD RESPONSE

As the structure-soil interface is selected at the top of the soil cement (+ 6 m), the free-field soil profile of the site consists of the layer of soil cement of 6 m thickness resting on bedrock.

To determine the free-field response of a site, the control motion, the control point in which this motion is assumed to act, and the wave pattern have to be specified. This is illustrated for the Koeberg site in Figure 4. The horizontal and vertical components of the control motion consist of artificial 30-s acceleration time-histories, the response spectra of which follow the US-NRC Regulatory Guide 1.60, normalized to 0.30 g and 0.20 g, respectively. The horizontal-response spectrum is shown for a damping ratio of 5% as a solid line in Figure 5. The control point is located at the top of the bedrock (0 m), without the

presence of the soil-cement. With respect to the total site (including the layer of soil-cement), the control motion thus acts at a fictitious rock outcrop. The free-field motion at the top of the soil-cement (+ 6 m) is determined for two different body-wave assumptions. The control motion is first deconvoluted to the halfspace (- 120 m), resulting in the amplitudes of the incident waves and then convoluted to the top of the soil cement. For vertically incident body waves the corresponding horizontal-response spectrum is plotted in Figure 5. For inclined body waves the angles of incidence of the P- and SV-waves ψ_P and ψ_{SV} in the halfspace are selected as 5° and 30°, resulting in apparent velocities of 7627 m/s and 5068 m/s, respectively. The corresponding amplitudes A_P and A_{SV} of the incident waves in the halfspace depend on both the horizontal and vertical components of the control motion. The horizontal-response spectrum for inclined body waves hardly differs from that for vertical incidence (Figure 5). This also applies to the vertical component (not shown). Besides assuming these two wave patterns, denoted as "vertical incidence" and "inclined waves" further on, a wave train consisting mainly of Rayleigh waves that results in the same motion at the top of the soil cement as the vertically incident body waves is also investigated, as described below. For a layered system the apparent velocity depends on the frequency. For the first two R-modes, the dispersion curves are shown in Figure 6. For frequencies above 9.1 Hz, where the second R-mode starts, the horizontal and vertical components of the motion at the top of the soil-cement can be associated with the two R-modes. For frequencies below 9.1 Hz, a P-wave with ψ_P= 5° (apparent velocity = 7627 m/s) is used in addition to the first R-mode. Details are discussed in Reference 4. This wave pattern is denoted as "R- and P-waves".
The analytical procedure is described in References 3 and 11.

4. SINGLE REACTOR BUILDING

For the sake of comparison, the single reactor building of the Koeberg nuclear-power plant, assumed to be founded on its own basemat on top of the soil-cement with Neoprene pads (without friction plates), is also investigated. To evaluate the influence of the aseismic bearings on the response, the same structure, but without the base isolation, is also examined.

Introducing the base isolation reduces the frequency of the first mode of the soil-structure system from 3.3 Hz to 0.9 Hz and that of the second from 6.6 Hz to 4.3 Hz. The horizontal component of the seismic input excites mainly the first mode for the isolated system while both modes contribute to the response for the rocking component (arising from horizontally propagating waves) (Ref.2).

The horizontal and vertical total accelerations in three points are specified for the reactor building with and without the base isolation in Table II. The favourable effect of the aseismic bearings on the horizontal response caused by vertically incident waves shown for comparison is clearly visible. The response caused only by the rocking seismic input motion of the R- and P-waves does not differ significantly for the two structures. This results in larger horizontally propagating wave effects on a percentage basis for the structure with the base isolation (taking the translational and rocking seismic input motions into account). The self-cancelling effect on the vertical response is small, as is visible in

Table II. The horizontal-response spectra are presented in Figure 7. For both structures the peaks at the frequencies of the first and second modes are clearly visible. The peak at 0.9 Hz of the base-isolated structure is not affected by horizontally propagating waves, while the second peak at 4.3 Hz is increased from 0.98 g to 2.13 g or by a factor 2.17 (top shield building). For the structure without base isolation the peak at 3.3 Hz is magnified from 24.8 g to 27.8 g or by a factor 1.12. As the seismic excitation forms only one of several load cases arising in the load combination governing design, the significance of these factors is limited (Ref. 2). Assuming e.g. that the contribution of the other load cases equals that of the seismic response of the structure without base isolation for vertical incidence (24.8 g) results in an increase of (24.8 + 27.8) / (24.8 + 24.8) = 1.06 for the structure without base isolation and of (24.8 + 2.13) / (24.8 + 0.98) = 1.04 for the base-isolated structure.

5. NUCLEAR ISLAND OF KOEBERG

The vibrational mode shapes of the linear system (omitting the friction plates) are useful when interpreting the dynamic behaviour. The first six modeshapes and the associated natural frequencies are shown in Figure 8. As expected, the structure with the upper raft moves (from a practical point of view) horizontally as a rigid body in the first mode.

To gain further insight into the different effects influencing the dynamic response, it is convenient to perform the analysis in two steps, the kinematic and inertial interactions.This decomposition remains computationally attractive, as the kinematic interaction part of the analysis is linear for this structural configuration.

The response spectra of the seismic input motion (resulting from the kinematic-interaction part of the analysis) are shown in Figure 9. The large dimension of the raft of the nuclear island leads to a stronger reduction of the horizontal component in the higher-frequency range than for the single reactor building shown for comparison (Figure 9a). Up to 10 Hz, the rocking input (multiplied by the same characteristic height = 30.8 m) is approximately the same for the three cases described in Figure 9b. Assuming the entire upper raft also to be rigid in the vertical direction results in a more pronounced diminution in the higher-frequency range.

The maximum total accelerations are shown in Table III for the nuclear island of Koeberg with Neoprene pads without and with friction plates for the various wave patterns. For vertical incidence the favourable influence of the Neoprene pads on the horizontal response leads to a small amplification with height. Adding friction plates reduces the horizontal accelerations even further. The differences in the horizontal response of the two reactor buildings for vertical incidence are small. They are caused by the second mode (among others) (Figure 8) which is excited by the vertical component of the seismic input. For the horizontally propagating R- and P-waves, the rotational seismic input results in an increase of the horizontal response throughout the structure. The differences for the reactor buildings discussed above are more pronounced. The inclined waves defined in Section 3 also increase the horizontal response compared to that for vertical incidence but, in general, less than for R- and P-waves.

In-structure response spectra for the nuclear island with Neoprene pads but without friction plates are presented in Figures 10 and 11 for the horizontal and vertical directions, respectively. The results for R- and P-waves are compared to those for vertical incidence. In the horizontal direction the peak at the frequency 0.89 Hz of the first mode is, as expected, dominant throughout the structures (Figure 10). The other peaks can also be associated with the frequencies of certain modes. The second mode, with a frequency 3.82 Hz (Figure 8), is easily detected at the top of the shield building and at the top of the internal structure. As expected from the mode shape, the peak is more pronounced for the horizontally propagating wave than for vertical incidence. The significant increase of the second peak at the top of the shield building also arises from the contribution of the third mode with a frequency 4.34 Hz. The fourth mode causes the peak at 7.15 Hz, clearly visible at the top of the internal structure. The peak for vertical incidence arises from the vertical seismic input. Modes 3, 5 and 6 are responsible for the peaks in the range between 4 and 10 Hz present for R- and P-waves at the top of the auxiliary building. In the vertical direction, horizontally propagating wave effects are small (Figure 11).

To study the influence of the vertical component of the seismic input motion on the horizontal response for vertically incident waves, the horizontal in-structure response spectrum on the upper raft is shown in Figure 12. As the upper raft of the symmetric structure is rigid horizontally, no such influence can exist in a linear system. Introducing friction plates and analysing for the horizontal component of the seismic input only, the favourable effect observed in the total horizontal acceleration in Table III is present in the response spectra throughout the frequency range (dashed versus dotted line in Figure 12). Adding the vertical component to the seismic motion, the favourable reduction of the peak at 0.89 Hz is unaffected (solid line). However, an additional peak arises at the frequency around 10 Hz, where the modes with large vertical-participation factors are located. This nonlinear coupling can be illustrated by examining the resultant of all horizontal Neoprene forces. Its time history is shown in Fig. 13 (horizontal and vertical components of seismic input for vertical incidence). The maximum permissible value of this resultant (calculated as the product of the vertical resultant of all Neoprene forces and of the friction coefficient) is also indicated. It depends on the vertical earthquake and would be constant for no vertical excitation. The high-frequency content of this maximum is imposed on the actual resultant horizontal Neoprene force during the time interval when all friction plates slide.

To evaluate the horizontally travelling wave effects on the in-structure response spectra for the nuclear island of Koeberg (with friction plates), the top of the shield building is selected. As can be seen from Figure 14, the spectra are similar to those shown for the linear system in Figure 10a. The increase for inclined waves (not shown) is somewhat smaller than for R- and P-waves. As discussed in connection with Figure 7b for the single reactor building, the impact of the large increase on a percentage basis is considerably reduced when load combinations are examined.

Finally, turning to the relative displacements, the time-history of the lower raft relative to the upper raft is plotted for vertical incidence in Figure 15. In addition the sliding displacements of the three Neoprene pads indicated by circles in Figure 2 are also shown. Because of the rocking motion of the reactor-building unit 2, the sliding starts at different times. The different sliding displacements result in residual horizontal Neoprene

forces present after the seismic excitation has died out. These are plotted for the 25 Neoprene pads for R- and P-waves and for vertical incidence in Figure 16. No tension arises vertically in the Neoprene pads during the complete seismic excitation for all wave patterns. A partial loss of contact thus does not occur.

6. CONCLUDING REMARKS

1. The nuclear island of Koeberg with a large basemat, a nonlinear base isolation effective in the horizontal direction only, founded on rock, is analysed for inclined body waves and for a combination of surface and body waves. The response is compared to that resulting from vertically incident waves.

2. Although the analysis of soil-structure interaction uses the principle of superposition by performing first the free-field analysis and then the actual interaction calculation, the structure in the latter can exhibit nonlinear behaviour. The governing equation of motion in the time domain contains convolution integrals, which can be removed by assuming a frequency-independent dynamic-stiffness matrix of the unbounded soil.

3. The horizontal and vertical components of the control motion are either associated with inclined P- and SV-waves or with a combination of a P-wave and the first two Rayleigh modes.

4. It is demonstrated that the aseismic bearings result in a significant isolation in the horizontal direction for vertically incident waves. The vertical excitation affects considerably the response in the horizontal direction in the frequency range of the vertical modes for the nonlinear base isolation.

5. When compared to vertical incidence,

   a) the horizontal component of the propagating wave is filtered significantly because of the size of the raft. However, this results in only a slightly smaller structural response, since the aseismic bearings already represent a filter;

   b) the vertical response is hardly affected by horizontally propagating waves;

   c) an additional rocking component arises, generated by the horizontally propagating vertical component. As the aseismic bearings do not isolate against this rocking component, the corresponding horizontal response bears comparison with that of a conventional structure. For the base-isolated structure, the rocking input leads to a considerable increase of the horizontal response;

   d) horizontally travelling waves hardly modify the maximum horizontal displacements and the amount and duration of sliding. A larger variation of the vertical Neoprene forces occurs, but no uplift arises.

6. Although the ratio of the response for horizontally propagating waves and that for vertically incident waves is considerably larger for the base-isolated structure than for a conventional one, the actual design incorporating other loading cases is affected much less.

Acknowledgment

The authors are indebted to the Electricity Supply Commission of South Africa and the Atomic Energy Board for permission to publish results of the study on horizontally propagating waves for the NPP Koeberg.

REFERENCES

1 J.P. Wolf and P. Obernhuber, "Effects of horizontally travelling waves in soil-structure interaction", Nucl. Eng. and Design, Vol. 57, 221 - 244 (1980).

2 J.P. Wolf and P. Obernhuber, "Effects of horizontally propagating waves on the response of structures with a soft first storey", Earthqu. Eng. Struct. Dyn., Vol. 9, 1 - 21 (1981).

3 J.P. Wolf and P. Obernhuber, "Free-field response from inclined SH-waves and Love-waves", Earthqu. Eng. Struct. Dyn., Vol. 10, 823-845 (1982).

4 J.P. Wolf and P. Obernhuber, "In-plane free-field response of actual sites", Earthqu. Eng. Struct. Dyn., to be published in Vol. 11 (1983).

5 C. Plichon, "Hooped rubber bearings and frictional plates - a modern anti-seismic engineering technique", The Anti-Seismic Design of Nuclear Installations, Proceedings of a Specialist Meeting, OECD, Paris, 1975.

6 F. Jolivet and M. Richli, "Aseismic foundation system for nuclear power stations", Trans. 4th Int. Conf. Struct. Mech. Reactor Tech., San Francisco, California, Paper K9/2 (1977)

7 C. Plichon and F. Jolivet, "Aseismic foundation systems for nuclear power plants", Engineering Design for Earthquake Environments, Institution of Mechanical Engineers Conference, London, Paper C190/78, 193 - 205 (1978).

8 U. Richli, N. Baur, J.F. Casagrande, "Effect of travelling waves on a shock isolated nuclear power plant put on rock foundation", Trans. 6th Int. Conf. Struct. Mech. Reactor Techn., Paris K12/7 (1981).

9 J.E. Luco, "Vibrations of a rigid disc on a layered viscoelastic medium", Nucl. Eng. and Design, Vol. 36, 325 - 340 (1976).

10 J.P. Wolf, G.R. Dabre, "Dynamic-stiffness matrix of surface foundation on layered halfspace based on stiffness-matrix approach", presented at Specialists' Meeting on Gas-Cooled Reactor Seismic Design Problems and Solutions, San Diego, California, Aug. 1982

11 J.P. Wolf and P. Obernhuber, "Free-field response from inclined SV- and P-waves and Rayleigh-waves", Earthqu. Eng. Struct. Dyn., Vol. 10, 847-869 (1982).

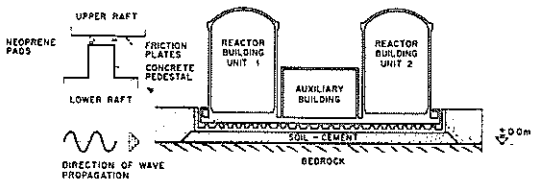

Fig. 1 Nuclear island on aseismic bearings of Koeberg Power Plant

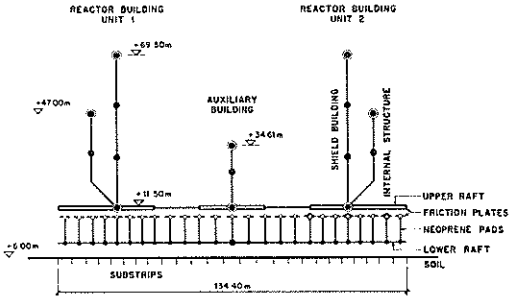

Fig. 2 Dynamic model of nuclear island of Koeberg

DEPTH [m]	SHEAR MODULUS [GN/m²]	DENSITY [Mg/m3]	SHEAR WAVE VELOCITY [m/s]	POISSON'S RATIO	DAMPING RATIO
+ 6.	1.17	2.15	733.	0.20	0.05
0.	3.00	2.60	1074.	0.35	0.03
- 5.	3.40	2.60	1144.	0.35	0.03
- 10.	5.00	2.60	1387.	0.40	0.03
- 20.	8.00	2.60	1754.	0.40	0.03
- 30.	12.00	2.60	2148.	0.40	0.03
- 40.	18.00	2.60	2631.	0.35	0.03
- 50.	27.00	2.60	3223.	0.30	0.03
- 60.	31.00	2.60	3453.	0.29	0.03
- 80.	38.50	2.60	3848.	0.27	0.03
-100.	46.00	2.60	4206.	0.26	0.03
-120.	50.00	2.60	4385.	0.25	0.03
∞					

Tab. I Free-field properties

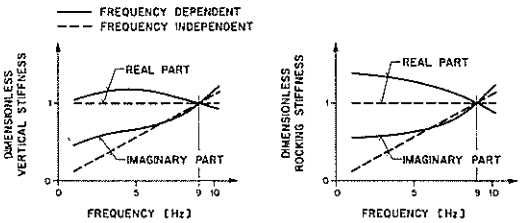

Fig. 3 Frequency dependency of dynamic stiffness of soil

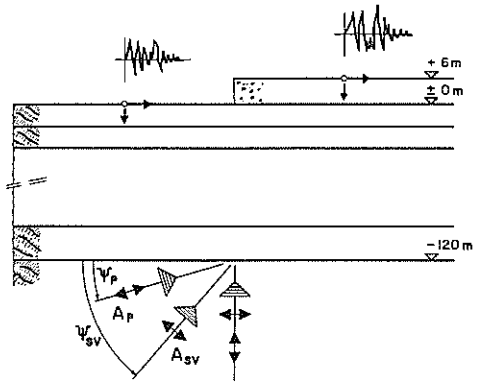

Fig. 4 Definition of seismic input

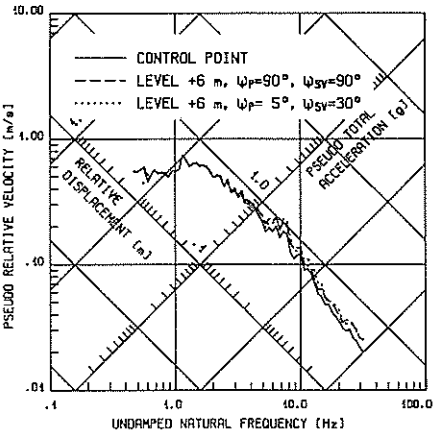

Fig. 5 Response spectra (5 % damping) of horizontal free-field motion

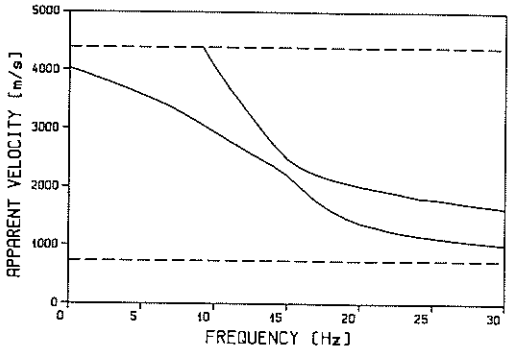

Fig. 6 Dispersion

	WITHOUT BASE ISOLATION			WITH BASE ISOLATION		
	VERTICAL INCIDENCE	R- AND P-WAVES		VERTICAL INCIDENCE	R- AND P-WAVES	
		ROCKING INPUT ONLY	COMPLETE INPUT		ROCKING INPUT ONLY	COMPLETE INPUT
HORIZONTAL:						
CENTRE BASEMAT	0.439	0.040	0.448	0.299	0.064	0.345
TOP SHIELD BUILDING	1.835	0.270	2.036	0.356	0.163	0.429
TOP INTERNAL STRUCTURE	1.182	0.152	1.264	0.318	0.112	0.392
VERTICAL:						
CENTRE BASEMAT	0.326		0.317	0.326		0.317
TOP SHIELD BUILDING	0.695		0.674	0.695		0.674
TOP INTERNAL STRUCTURE	0.376		0.364	0.376		0.364

Tab. II Maximum total acceleration [g], single reactor building

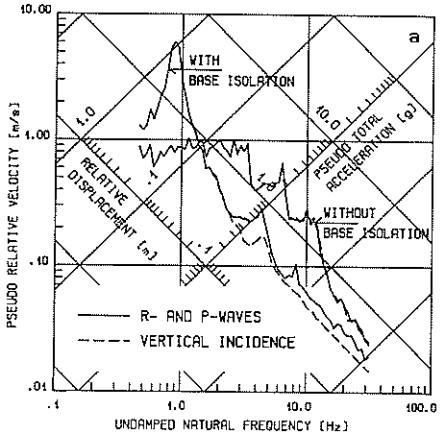

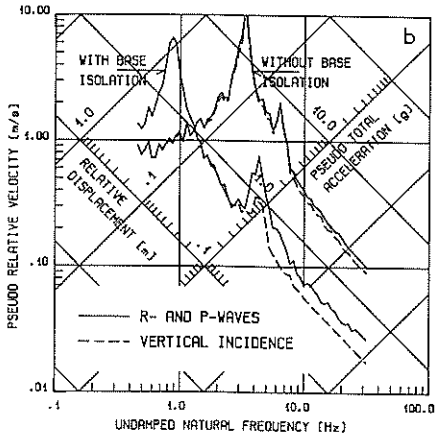

Fig. 7 Horizontal in-structure response spectra (2 % damping), single reactor building
a) centre basemat b) top shield building

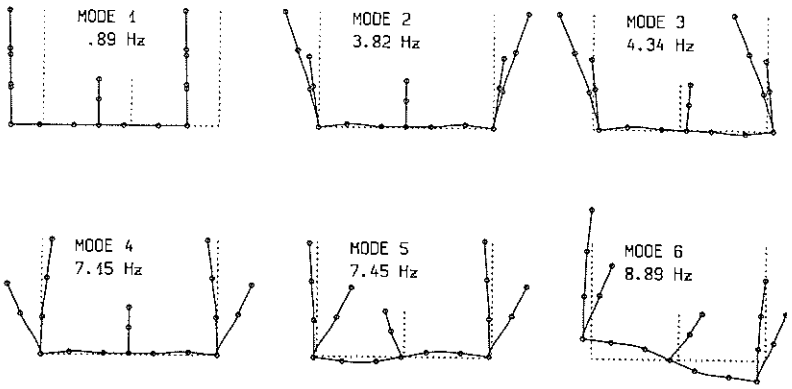

Fig. 8 Mode shapes and natural frequencies, nuclear island of Koeberg

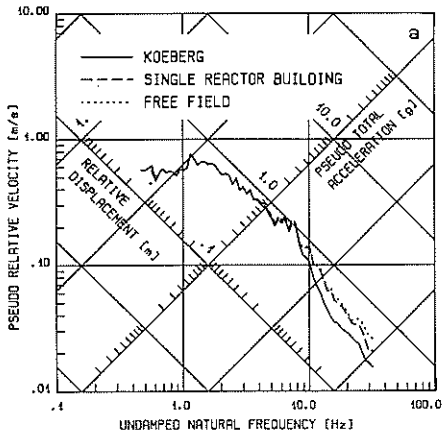

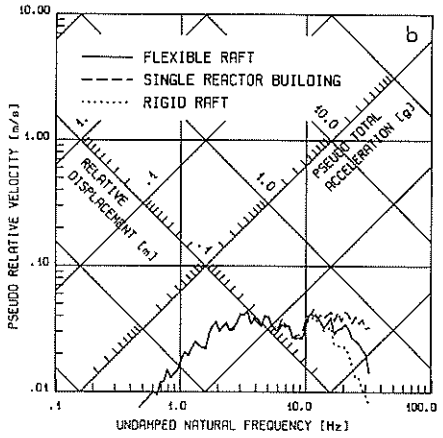

Fig. 9 Response spectra (5 % damping) of seismic-input motion, nuclear island of Koeberg, R- and P-waves
a) horizontal b) rocking * 30.8 m, reactor building unit 1

	WITHOUT FRICTION PLATES		WITH FRICTION PLATES		
	VERTICAL INCIDENCE	R- AND P-WAVES	VERTICAL INCIDENCE	R- AND P-WAVES	INCLINED WAVES
HORIZONTAL:					
UPPER RAFT	0.304	0.338	0.186	0.189	0.198
TOP SHIELD BUILDING UNIT 1	0.388	0.528	0.252	0.425	0.337
TOP INTERNAL STRUCTURE UNIT 1	0.369	0.508	0.251	0.312	0.322
TOP SHIELD BUILDING UNIT 2	0.355	0.451	0.255	0.326	0.307
TOP INTERNAL STRUCTURE UNIT 2	0.380	0.397	0.279	0.304	0.257
TOP AUXILIARY BUILDING	0.310	0.386	0.252	0.269	0.275
VERTICAL:					
CENTRE UPPER RAFT UNIT 1	0.301	0.303	0.301	0.303	0.334
CENTRE UPPER RAFT UNIT 2	0.284	0.295	0.284	0.295	0.300
CENTRE UPPER RAFT AUXILIARY BUILDING	0.302	0.284	0.302	0.285	0.310

Tab. III Maximum total acceleration [g], nuclear island of Koeberg

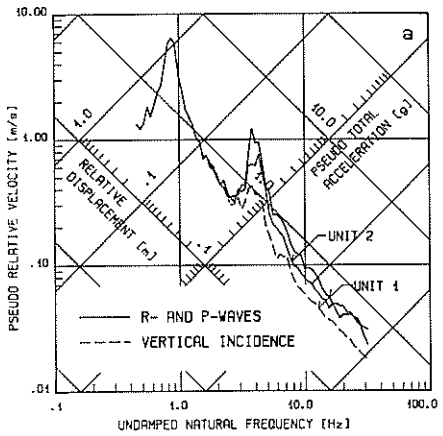

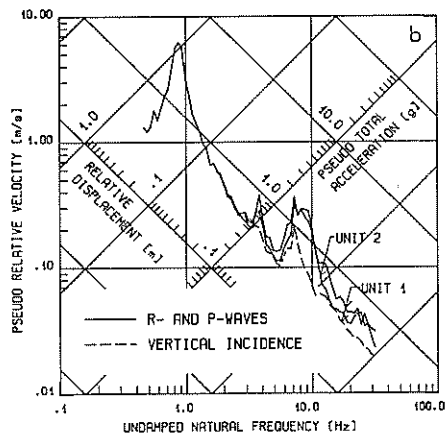

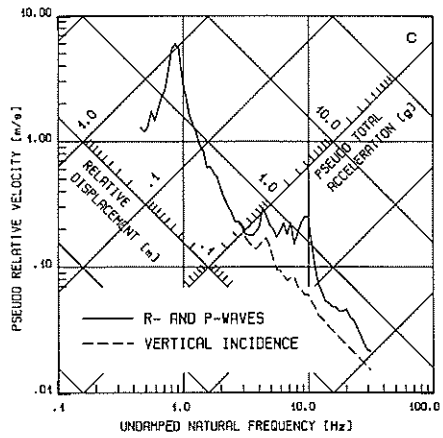

Fig. 10 Horizontal in-structure response spectra (2 % damping), nuclear island of Koeberg without friction plates
a) top shield building b) top internal structure c) top auxiliary building

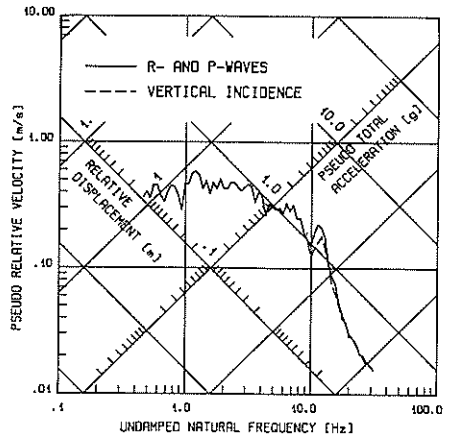

Fig. 11 Vertical in-structure response spectra (2 % damping), nuclear island of Koeberg without friction plates, base auxiliary building

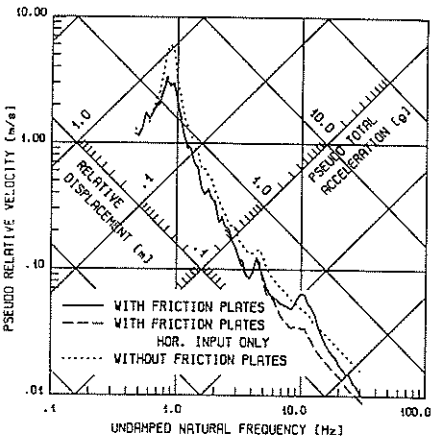

Fig. 12 Horizontal in-structure response spectra (2 % damping), nuclear island of Koeberg, upper raft

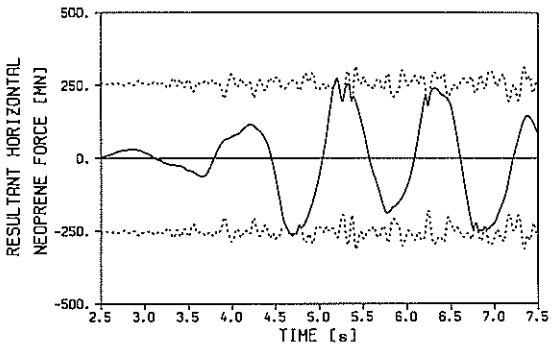

Fig. 13 Time-history of resultant horizontal Neoprene forces, nuclear island of Koeberg, vertical incidence

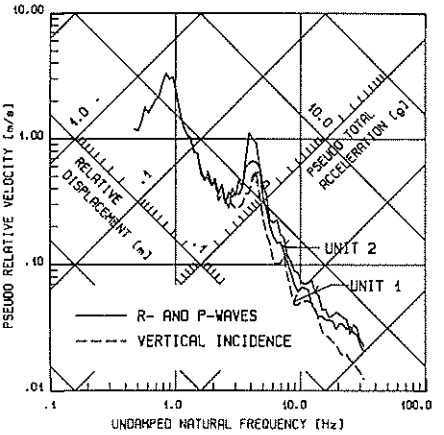

Fig. 14 Horizontal in-structure response spectra (2 % damping), nuclear island of Koeberg, top shield building

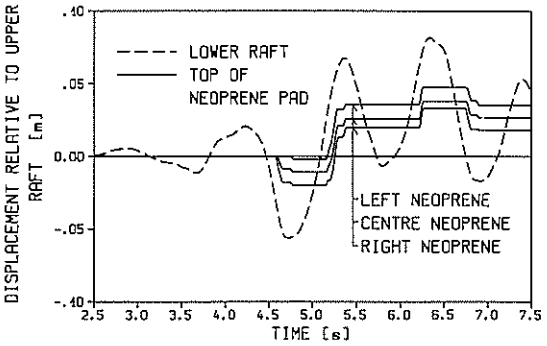

Fig. 15 Time-history of horizontal relative displacements, nuclear island of Koeberg, reactor building unit 2, vertical incidence

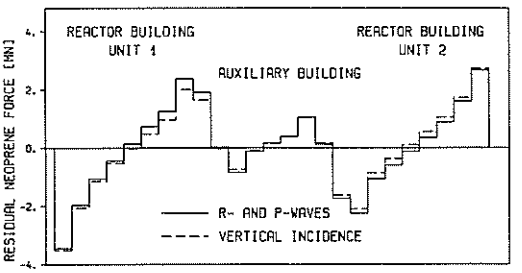

Fig. 16 Residual horizontal Neoprene forces, nuclear island of Koeberg